Fokker-Planck simulation for radial transport of high energy ions

K.Hamamatsu, N.Hayashi, T.Takizuka, T.Ozeki

Japan Atomic Energy Agency,
801-1 Mukohyama, Naka, Ibaraki, 311-0193, JAPAN
hamamatsu.kiyotaka@jaea.go.jp

abstract : The radial transport term is modelled in the bounce averaged Fokker-Planck equation. The distribution function of fast ions by NBI is numerically analyzed by the bounce averaged Fokker-Planck equation with a radial diffusion coefficient modelled by a function of velocity. The obtained results are compared with the results of an orbit following Monte Carlo code.

1. Introduction

The development of the transport model for high-energy ions is one of the most important issues in simulation studies of burning plasmas. One of effective models is a Monte-Carlo(MC) simulation, where orbits of many test ions are numerically integrated and velocity scatterings due to the Coulomb collisions are simulated by the MC technique. As typical numerical codes, F3D-OFMC[1, 2], and ASCOT[3] ,etc., have been developed. The MC model can analyze effects of the toroidal ripple field on the radial transport and on the local heat load on a 3-dimensional first wall. The MC simulations, however, need huge amounts of CPU time to treat a huge number of test particles for the reduction of statistical noise. Due to the above huge computational resources, it is not easy to perform the MC simulation with other time-dependent simulations, e.g., a transport simulation of the bulk plasma.

As another approach, the time evolution of velocity distribution function is obtained by solving the Fokker-Planck(FP) equation. In an axi-symmetric configuration, especially, the bounce averaged FP(BAFP) equation[4] expresses the orbit effects without finite banana size effects. Since the BAFP equation describe the behavior of high-energy ions in the bulk plasma, various BAFP codes have been developed for many issues because of very cheep computational cost. These BAFP codes have been incorporated into other numerical codes. We have developed the FP-RAT code[5], which is the solver of the FP equation with the radial transport in the (v, ρ)-space, and incorporated into the TOPIC-IB (TOPICS extended in Integrated simulation for Burning plasma) code[6]. However, a radial transport term in the BAFP equation has not yet well been discussed.

In this study, we formulate the BAFP equation with the modelled radial transport term by using a relation between bounce average and flux surface average. The velocity distribution function is numerically obtained by solving the formulated BAFP equation with a modelled radial transport coefficient. The obtained results are compared with the results of MC model.

2. Bounce averaged FP equation with radial transport

To discuss the modelling of the radial transport term in the BAFP equation, this section is started from the review of conventional theory.

2.1 Bounce averaged FP equation

We introduce the distribution function $f(\rho, \boldsymbol{v}, t)$ and the following FP equation:

$$\frac{\partial f}{\partial t} = C(f) + S_{\rm p} + L_{\rm th} + R(f), \tag{1}$$

where C the Coulomb collision term, $S_{\rm p}$ the particle source term, $L_{\rm th}$ is the loss term of slowed down particles, and the last term R shows a radial transport. When the magnetic flux surface coordinates (ρ, θ, ζ), where $\rho \in [0, 1]$ the label of flux surface, θ the poloidal angle and ζ is the toroidal angle, respectively, are introduced, the magnetic field $\boldsymbol{B}$ is expressed as $\boldsymbol{B} = \psi'_{\rm p}(\rho)\boldsymbol{\nabla}\zeta \times \boldsymbol{\nabla}\rho + B_{\rm T}(\psi_{\rm p})\boldsymbol{\nabla}\zeta$, where $\psi_{\rm p}$ is the poloidal magnetic flux, and $\psi'_{\rm p} = {\rm d}\psi_{\rm p}/{\rm d}\rho$, $B_{\rm T}$ is the toroidal magnetic field multiplied by the major radius.

The convective term due to particle motion along the magnetic field line for the distribution function, i.e., $\boldsymbol{v}_{\parallel}\cdot\boldsymbol{\nabla} f$, is written as

$$v\cos\eta \boldsymbol{b}\cdot\boldsymbol{\nabla} f = \frac{v\cos\eta}{\mathcal{L}}\frac{\partial f}{\partial \theta}, \tag{2}$$

where η is the pitch angle of particle velocity. The line element along the field line, $\mathcal{L}$, is given by

$$\mathcal{L} = \frac{\sqrt{g}}{\mathcal{A}_\theta}, \qquad \mathcal{A}_\theta = \frac{\psi'_{\rm p}}{B}, \tag{3}$$

where $\mathcal{A}_\theta$ is the area element associated to $\mathcal{L}$ and $\sqrt{g} = 1/(\boldsymbol{\nabla}\rho\cdot(\boldsymbol{\nabla}\theta\times\boldsymbol{\nabla}\zeta))$ is the Jacobian. When the poloidal angle where B is at minimum on the flux surface, ρ, is shown by θ_0 and also the pitch angle is shown by η_0, the pitch angle at poloidal position θ can be given by the energy conservation (v_0 is constant) and the adiabatic invariance of magnetic moment, i.e.,

$$\sin^2\eta(\rho,\theta) = \psi_{\rm B}(\rho,\theta)\sin^2\eta(\rho,\theta_0), \tag{4}$$

where $\psi_{\rm B}(\rho,\theta) = B(\rho,\theta)/B(\rho,\theta_0)$. The eq.(4) determines a periodic motion of trapped or transit particle motion along the field line. From the eq.(2), the period of bounce motion, $\tau_{\rm B}$, is evaluated as

$$\tau_{\rm B} = \oint \frac{\mathcal{L}(\rho,\theta){\rm d}\theta}{|v_{\parallel}|}. \tag{5}$$

When the characteristic length of orbit, λ, is defined by

$$\lambda = \oint \frac{|\cos\eta_0|}{|\cos\eta|}\mathcal{L}{\rm d}\theta, \tag{6}$$

the bounce time is expressed as $\tau_{\rm B} = \lambda/(v_0\cos\eta_0)$. Along this periodic motion, the bounce average operator for any function $X(\rho,\theta)$ is defined by

$$\langle X\rangle_{\rm B} = \frac{1}{\tau_{\rm B}}\oint X\frac{\mathcal{L}{\rm d}\theta}{|v_{\parallel}|} = \frac{1}{\lambda}\oint X\frac{|\cos\eta_0|}{|\cos\eta|}\mathcal{L}{\rm d}\theta. \tag{7}$$

When we consider that the bounce time is much shorter than the collision time and the radial transport time, the distribution function can be ordered as $f(\rho,\theta,v,\eta,t) = f_0(\rho,\theta_0,v_0,\eta_0,t) + \epsilon f_1(\rho,\theta(t_{\rm B}),v_0,\eta(t_{\rm B}),t,t_{\rm B})$, where $t_{\rm B}$ is the time of bounce motion, i.e.,

$0 \leqq t_{\rm B} \leqq \tau_{\rm B}$, and ϵ is a smallness parameter. By operating bounce average to the eq.(1) we obtain the BAFP equation for f_0:

$$\frac{\partial \lambda f_0}{\partial t} = \lambda \langle C(f_0) \rangle_{\rm B} + \lambda \langle S_{\rm p} \rangle_{\rm B} + \lambda \langle L_{\rm th} \rangle_{\rm B} + \lambda \langle R(f_0) \rangle_{\rm B}. \tag{8}$$

The bounce averaged Coulomb collision operator has been obtained in the ref.[4], i.e.,

$$\begin{aligned} \lambda \langle C(f_0) \rangle_{\rm B} &= -\frac{1}{v_0^2}\frac{\partial}{\partial v_0}\left[-D_{vv0}\frac{\partial f_0}{\partial v_0} - D_{v\eta 0}\frac{1}{v_0}\frac{\partial f_0}{\partial \eta_0} + F_{v0} f_0\right] \\ &\quad -\frac{1}{v_0 \sin\eta_0}\frac{\partial}{\partial \eta_0}\left[\sin\eta_0\left(-D_{\eta v0}\frac{\partial f_0}{\partial v_0} - D_{\eta\eta 0}\frac{1}{v_0}\frac{\partial f_0}{\partial \eta_0} + F_{\eta 0} f_0\right)\right], \end{aligned} \tag{9}$$

where the bounce averaged coefficients are:

$$\begin{aligned} &D_{vv0} = \lambda \langle D_{vv} \rangle_{\rm B}, \quad && D_{v\eta 0} = \lambda \left\langle \frac{\tan\eta_0}{\tan\eta} D_{v\eta} \right\rangle_{\rm B}, \quad && F_{v0} = \lambda \langle F_v \rangle_{\rm B}, \\ &D_{\eta v0} = \lambda \left\langle \frac{\tan\eta_0}{\tan\eta} D_{\eta v} \right\rangle_{\rm B}, \quad && D_{\eta\eta 0} = \lambda \left\langle \frac{\tan^2\eta_0}{\tan^2\eta} D_{\eta\eta} \right\rangle_{\rm B}, \quad && F_{\eta 0} = \lambda \left\langle \frac{\tan\eta_0}{\tan\eta} F_{\eta} \right\rangle_{\rm B}. \end{aligned} \tag{10}$$

2.2 Modelling of radial transport term

Before modelling of the radial transport term, we consider the particle number in the shell $[\rho, \rho + {\rm d}\rho]$. The area ${\rm d}S_{\theta 0}$ at $\theta = \theta_0$ is expressed by

$${\rm d}S_{\theta 0} = \frac{\sqrt{g}_{\theta=\theta_0} {\rm d}\rho {\rm d}\theta {\rm d}\zeta}{\mathcal{L}(\rho, \theta_0) {\rm d}\theta} = \mathcal{A}_{\theta 0} {\rm d}\rho {\rm d}\zeta. \tag{11}$$

The particles in the volume element ${\rm d}^3\boldsymbol{v}_0$, which are passing through the area at $\theta = \theta_0$ with the parallel velocity $v_0 \cos\eta_0$, return back to $\theta = \theta_0$ after the bounce time $\tau_{\rm B}$. The particle number ${\rm d}\mathcal{N}(\rho, v_0, \eta_0)$ in the shell $[\rho, \rho + {\rm d}\rho]$ is evaluated by

$${\rm d}\mathcal{N}(\rho, v_0, \eta_0) = \oint_{\zeta=0}^{\zeta=2\pi} \tau_{\rm B} v_0 \cos\eta_0 f_0(\rho, v_0, \eta_0) {\rm d}\boldsymbol{v}_0 {\rm d}S_{\theta 0} = 2\pi\lambda \mathcal{A}_{\theta 0}(\rho) f_0(\rho, v_0, \eta_0) {\rm d}\boldsymbol{v}_0 {\rm d}\rho. \tag{12}$$

Next we consider the flux surface (FS) average of $f_0 {\rm d}^3\boldsymbol{v}$[7], where ${\rm d}^3\boldsymbol{v}$ is related to ${\rm d}^3\boldsymbol{v}_0$ by the eq.(3), i.e.,

$${\rm d}^3\boldsymbol{v} = \psi_{\rm B} \frac{|\cos\eta_0|}{|\cos\eta|} {\rm d}^3\boldsymbol{v}_0. \tag{13}$$

According to the definition of FS average:

$$\left\langle f_0 {\rm d}^3\boldsymbol{v} \right\rangle_{\rm M} = \frac{1}{V'} \oint \sqrt{g} {\rm d}\theta {\rm d}\zeta f_0 {\rm d}^3\boldsymbol{v}, \quad V' = \oint \sqrt{g} {\rm d}\theta {\rm d}\zeta, \tag{14}$$

the relation between bounce- and flux surface average:

$$\left\langle f_0 {\rm d}^3\boldsymbol{v} \right\rangle_{\rm M} = \frac{2\pi}{V'} \frac{\psi_{\rm p}'}{B(\rho, \theta_0)} \left(\oint f_0 \frac{|\cos\eta_0|}{|\cos\eta|} \frac{B\sqrt{g}}{\psi_{\rm p}'} {\rm d}\theta \right) {\rm d}^3\boldsymbol{v}_0 = \frac{2\pi\lambda\mathcal{A}_{\theta 0}}{V'} \langle f_0 \rangle_{\rm B} {\rm d}^3\boldsymbol{v}_0. \tag{15}$$

is obtained. And by using the eq.(12), we can write as

$$\left\langle f_0 \mathrm{d}^3\boldsymbol{v} \right\rangle_{\mathrm{M}} = \frac{\partial \mathcal{N}}{\partial V}. \tag{16}$$

This equation means that the FS average of $f_0 \mathrm{d}^3\boldsymbol{v}$ is the particle number density on the ρ-surface.

From the above consideration, we assume the density variation by the radial transport on the ρ-surface as

$$\left.\frac{\partial}{\partial t}\left(\frac{\partial \mathcal{N}}{\partial V}\right)\right|_{\mathrm{R}} = \left\langle \boldsymbol{\nabla}\cdot(\boldsymbol{\Gamma}\mathrm{d}^3\boldsymbol{v}) \right\rangle_{\mathrm{M}}, \tag{17}$$

where $\boldsymbol{\Gamma}$ is a particle flux due to the radial transport. Since the RHS term can be rewritten as

$$\left\langle \boldsymbol{\nabla}\cdot(\boldsymbol{\Gamma}\mathrm{d}^3\boldsymbol{v}) \right\rangle_{\mathrm{M}} = \frac{\partial}{\partial V}\left\langle \boldsymbol{\Gamma}\cdot\boldsymbol{\nabla}V \mathrm{d}^3\boldsymbol{v} \right\rangle_{\mathrm{M}}. = \frac{\partial}{\partial V}\left(2\pi\lambda\mathcal{A}_{\theta 0}\langle \boldsymbol{\Gamma}\cdot\boldsymbol{\nabla}\rho\rangle_{\mathrm{B}}\right)\mathrm{d}^3\boldsymbol{v}_0, \tag{18}$$

the eq.(17) is transformed into

$$\left.\frac{\partial \lambda\mathcal{A}_{\theta 0} f_0}{\partial t}\right|_{\mathrm{R}} = \frac{\partial}{\partial \rho}\left(\lambda\mathcal{A}_{\theta 0}\langle \boldsymbol{\Gamma}\cdot\boldsymbol{\nabla}\rho\rangle_{\mathrm{B}}\right). \tag{19}$$

When the radial flux is assumed to consist of diffusion and convection, i.e., $\boldsymbol{\Gamma} = \boldsymbol{D}(\boldsymbol{v})\cdot\boldsymbol{\nabla}f_0 + \boldsymbol{V}(\boldsymbol{v})f_0$ with $\boldsymbol{D} = D_{\rho\rho}\boldsymbol{\nabla}\rho\boldsymbol{\nabla}\rho$ and $\boldsymbol{V} = V_\rho\boldsymbol{\nabla}\rho$, the radial flux is expressed as

$$\boldsymbol{\Gamma} = \left(-g^{\rho\rho}D_{\rho\rho}\frac{\partial f_0}{\partial \rho} + V_\rho f_0\right)\boldsymbol{\nabla}\rho = \left(-D\frac{\partial f_0}{\partial \rho} + \frac{V}{|\boldsymbol{\nabla}\rho|}f_0\right)\boldsymbol{\nabla}\rho, \tag{20}$$

where the dimension of D is L^2/T and one of V is L/T. As the result of our consideration, we show the BAFP equation with the modelled radial transport term :

$$\frac{\partial \lambda\mathcal{A}_{\theta 0} f_0}{\partial t} = \lambda\mathcal{A}_{\theta 0}\langle C(f_0)\rangle_{\mathrm{B}} + \lambda\mathcal{A}_{\theta 0}\langle S_{\mathrm{p}}\rangle_{\mathrm{B}} - \lambda\mathcal{A}_{\theta 0}\langle L_{\mathrm{th}}\rangle_{\mathrm{B}} + \frac{\partial}{\partial \rho}\left[\lambda\mathcal{A}_{\theta 0}\left(-D_0\frac{\partial f_0}{\partial \rho} + V_0 f_0\right)\right], \tag{21}$$

where $D_0 = \left\langle |\boldsymbol{\nabla}\rho|^2 D(\boldsymbol{v}) \right\rangle_{\mathrm{B}}$ and $V_0 = \langle |\boldsymbol{\nabla}\rho| V(\boldsymbol{v})\rangle_{\mathrm{B}}$. This equation is expressed by a conservation form, which is suitable for numerical analysis.

2.3 Modelling of radial transport coefficient

We examine a neoclassical-type transport as a first step. Therefore a convection term $\boldsymbol{V}$ is neglected and $D(\boldsymbol{v})$ is assumed to depend only on $\boldsymbol{v}_0$ at $\theta = \theta_0$,

$$D_0 = \left\langle |\boldsymbol{\nabla}\rho|^2 \right\rangle_{\mathrm{B}} D(v_0, \eta_0). \tag{22}$$

The diffusion coefficient D may show different feature in trapped- and transit-particle region. The modelled D is assumed as

$$D(v_0, \eta_0) = D_{\mathrm{C}} \times \begin{cases} \nu_{\mathrm{D}}(v_0, \eta_0)\Delta_{\mathrm{B}}^2, & \text{for trapped particle} \\ \\ \nu_{\mathrm{D}}(v_0, \eta_0)\Delta_{\mathrm{T}}^2, & \text{for transit particle} \end{cases} \tag{23}$$

where $\Delta_{\rm B} = 2v_{\|0}/\Omega_{\rm p0}$ is the banana width, $\Delta_{\rm T} = qv/\Omega_0$ is the eccentricity of drift orbit and q is the safety factor. Since the diffusion increases with an increase of collision frequency and an effective step-size increases with an increase of bounce frequency, the diffusion frequency is evaluated by the geometric mean of the pitch angle scattering frequency, ν_η, and the bounce frequency $\nu_{\rm B} = 1/\tau_{\rm B}$, i.e., $\nu_{\rm D} = \sqrt{\nu_{\rm B}\nu_\eta}$. Here, the velocity dependence of ν_η is expressed by

$$\nu_\eta(v) = \sum_s \frac{\gamma_s}{v^3}\left[\left(2 - \frac{1}{u^2}\right)\mathrm{erf}(u) + \frac{\mathrm{erf}'(u)}{u}\right], \quad u = \frac{v}{v_{{\rm t}s}}, \quad \gamma_s = \frac{n_s q_s^2 q_{\rm D}^2 \ln\Lambda}{4\pi\epsilon_0 m_{\rm D}}, \tag{24}$$

where s shows the s-th particle species, $v_{{\rm t}s}$ is the thermal velocity, and erf is the error function. The dimensionless constant $D_{\rm C}$ is treated as a given parameter in the following numerical analyses.

3. Numerical analyses

The purpose of this section is check of accuracy of the solution obtained by the eq.(21) with the diffusion coefficient of the eq.(23). We compare the numerical solutions of the eq.(21) with the results obtained by the MC model. Since the MC model gives the steadstate solution, the time evolution of the eq.(21) is also followed to the steady state.

The numerical analysis is carried out for fast ions by NBI in a plasma of JT-60SA class tokamak, i.e., $B_{\rm t} \simeq 2.5$T, $I_{\rm p} \simeq 3.5$MA, $R_0 \simeq 3.1$m, $a \simeq 0.9$m. The MHD equilibrium is fixed with normal q-profile, as shown in Fig.1(a). The bulk plasma is composed of

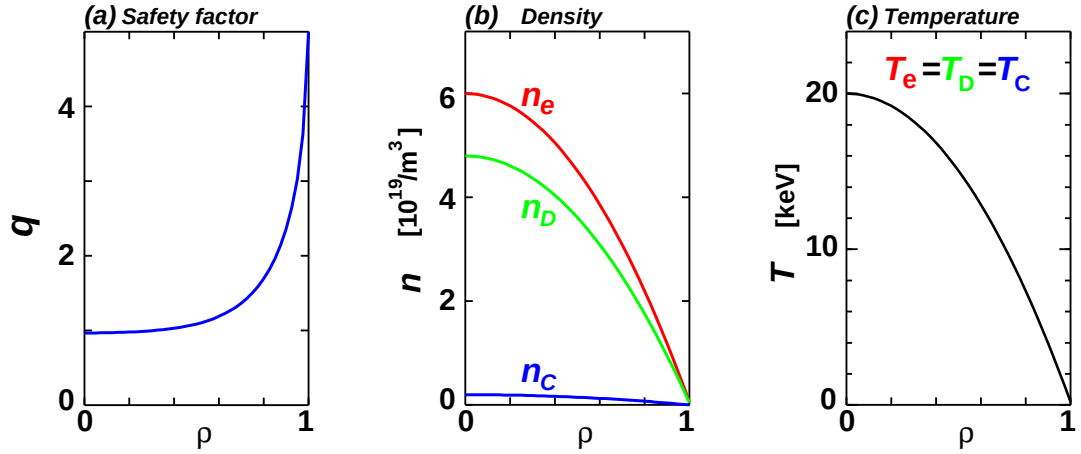

Fig.1. Radial profiles. (a) is safety factor, (a) is density, (c) is temperature.

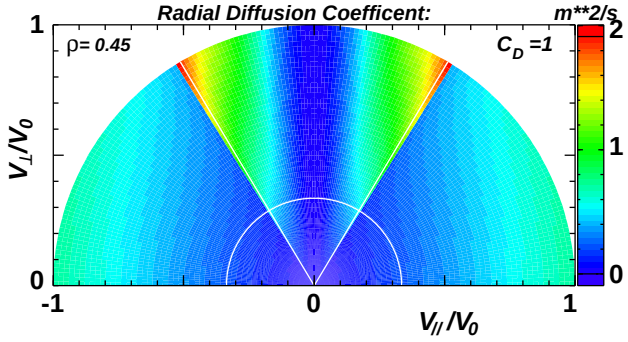

Fig.2. Radial diffusion coefficient with $C_{\rm D} = 1$ at $\rho = 0.45$

deuterium, carbon and electron, whose radial profiles of density and temperature are also fixed as shown in Fig.1(b) and (c). The radial diffusion coefficient given by the eq.(23) with $D_{\rm C} = 1$ at $\rho = 0.45$ is shown in Fig.2, where the velocity is normalized by $V_0 = \sqrt{2 \times 140{\rm keV}/m_{\rm D}}$. In the figure, two white lines show the boundaries between trapped- and transit particle region and white semicircle shows the thermal velocity of bulk deuterium.

The deuterium NB is injected with the energy 100keV and the power 10MW. The top-view of the beam line is illustrated in Fig.2 (a) and the intensity of power deposition on the poloidal plane is shown in Fig.2(b). The birth profile of fast ions along the ρ-direction is shown in Fig.2(c), where the birth of trapped particles is shadowed.

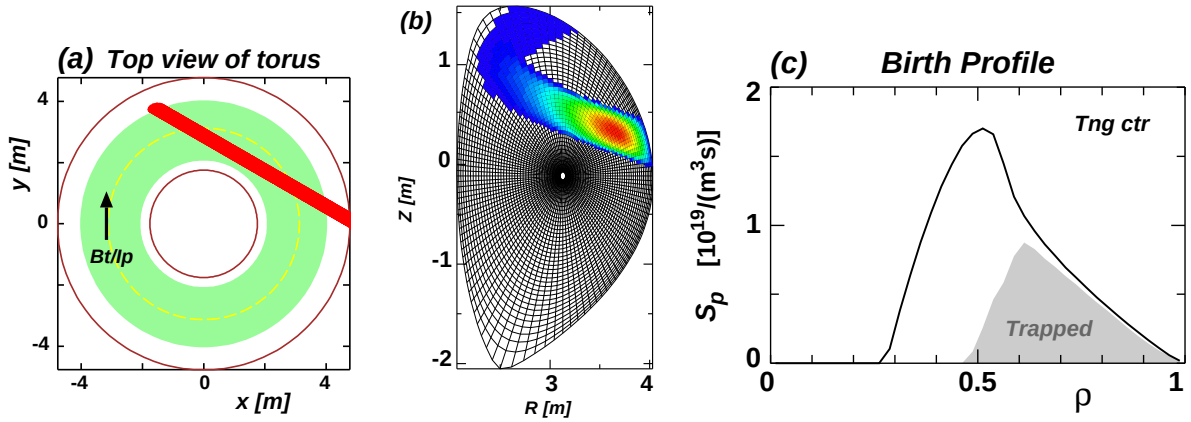

Fig.2. (a) shows top view of beam line. (b) shows power deposition on poloidal plane. (c) shows birth profile of fast ion.

The time evolution of distribution function, f_0, is traced by the BAFP equation (21) and goes into the steady state after $t \simeq 1$s. The Fig.3(a) shows the particle source, $\langle S_{\rm p} \rangle_{\rm B}$, in the velocity space at $\rho \simeq 0.5$. The Fig.3(b) illustrates f_0 at the same radial position of (a) with $D_{\rm C} = 1$. The distribution function is suddenly reduced below the thermal velocity, shown by the white semicircle, by the loss term, $L_{\rm th}$, in the eq.(21). In this numerical analysis, the radial mesh size $N_\rho = 40$, the velocity one $N_v = 50$, and the pitch angle one $N_\eta = 180$ are used.

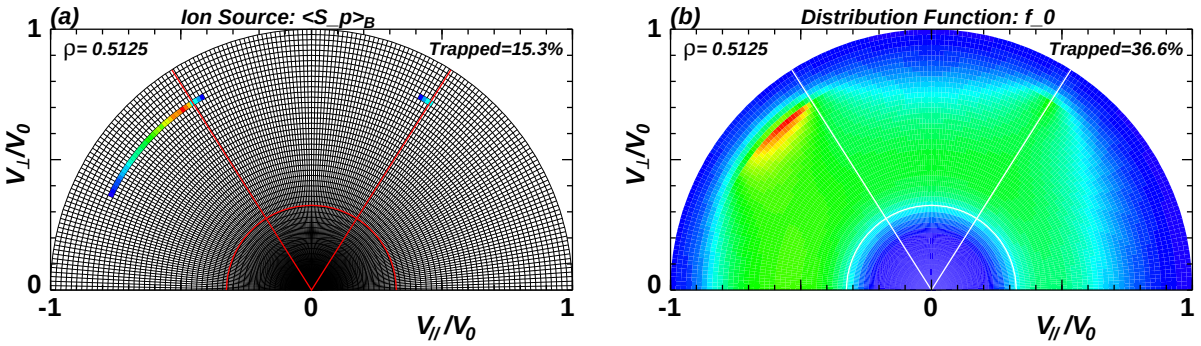

Fig.3. Distribution in velocity space at $\rho \simeq 0.5$. (a) shows birth profile of fast ions. (b) shows distribution function.

The Figure 4 shows the radial profiles of fast ion density in (a) and pressure in (b). In this figure, the dependence of dimensionless constant $D_{\rm C}$ is examined. The black

curves show the case of $D_C = 0$, which means all fast ions are slowed down at their birth positions. The green and blue curves show the cases of $D_C = 1$ and $= 4$, respectively. The red curves are obtained by the MC model with 10^5 test particles,

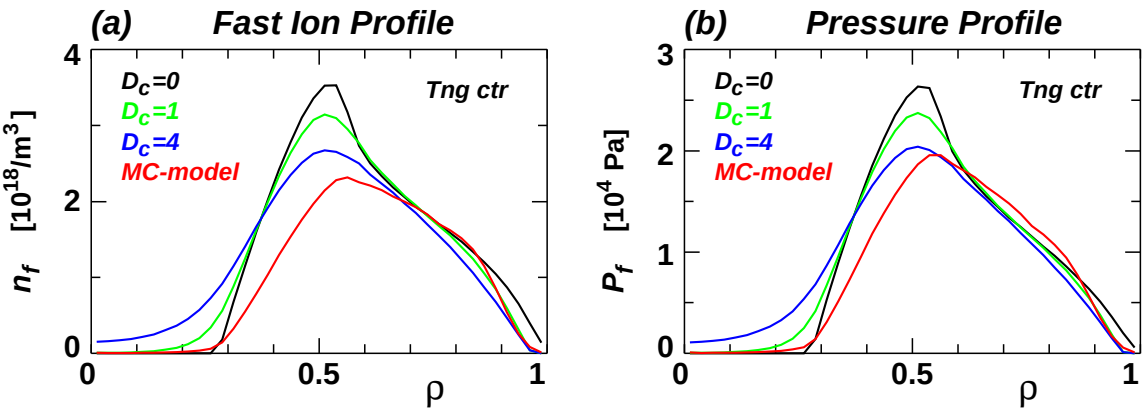

Fig.4 Radial profiles. (a) is the fast ion particle density. (b) is the fast ion pressure.

4. Summary and discussions

The bounce averaged FP equation with the modelled radial transport term is formulated by assuming that the flux surface average of the divergence term expresses the density variation due to the radial transport. As a first step, by using the radial diffusion coefficient assumed to be a function of particle velocity, the distribution function of fast ion by NBI is numerically analyzed and compared with the results of MC model.

When the free parameter D_C is varied, the radial profiles of fast ion and pressure tend to close the results of MC model. The reason why the peak position of radial profiles of the BAFP results shifts from the peak position of the MC model results may be because the effect of finite banana size is omitted in the numerical evaluation of the birth profile. The finite orbit effects on the birth profile will be included in the next step.

In this study, the radial diffusion coefficient is given as a function of velocity. However, the neoclassical transport comes from the pitch angle scattering in the velocity space caused by the Coulomb collisions. The modelling of radial transport related to the Coulomb collision operator is in our future planning.

5. Acknowledgement

The authors are grateful to Mr. M-N.Suzuki for computational support. This work was supported in part by the Grant-in-Aid for Scientific Research from Japan Society for the Promotion of Science (JSPS).

References

[1] Tani, K., et al, J. Phys. Soc. Japan **50**(1981)1726

[2] Shinohara, K., et al, Nuclear Fusion **43**(2003)586

[3] Heikkinen, J.A. and Sipila S.K. Comput. Phys. Commun. **76**(1993) 215

[4] Killeen, J. et al, *Computational Methods for Kinetic Models of Magnetically Confined Plasmas*, Springer-Verlag, New York, 1986

[5] Hamamatsu, K. et al, *Proceedings of the 10th IAEA TM on Energetic Particles in Magnetic Confinement Systems*, IAEA, 2010

[6] HAYASHI, N., et.al., Nucl.Fusion **47**(2007)682.

[7] Harvey, R.W. and McCoy, M.G. *The CQL3D Fokker-Planck Code*, http://www.compxco.com/050520_cql3d_manual.pdf